Copolyfluorenes Containing Bipolar Groups: Synthesis and Application To Enhance Electroluminescence of MEH−PPV

Chia-Shing Wu and Yun Chen*

Department of Chemical Engineering, National Cheng Kung University, Tainan, Taiwan

Received March 3, 2009; Revised Manuscript Received April 7, 2009

ABSTRACT: Enhancing electroluminescence of conventional MEH−PPV {poly[2-methoxy-5-(2′-ethylhexyloxy)-1,4-phenylenevinylene]} is desirable due to its popularity in polymeric emitting materials. The enhancement is much readily attained by simple blending with functional polymers instead of tedious structural modification. In response to this, three copolyfluorenes (**P1**−**P3**) containing bipolar groups (3.1−11.2 mol %), directly linked hole-transporting triphenylamine and electron-transporting 1,2,4-triazole, are synthesized by Suzuki coupling reaction. The bipolar groups not only suppress undesirable green emission of polyfluorene under thermal annealing but also increase hole and electron affinity of the resulting copolyfluorenes. Blending the bipolar copolyfluorenes with MEH−PPV effectively improves the emission efficiency of its electroluminescent devices [ITO/PEDOT:PSS/polymer blend/Ca(50 nm)/Al(100 nm)]. The maximum luminance and maximum luminance efficiency are significantly enhanced from 3120 cd/m^2 and 0.49 cd/A (MEH−PPV device) to 19 560 cd/m^2 and 1.08 cd/A (blend device with ca. 0.5 wt % of bipolar groups), respectively. Our results demonstrate the efficacy of the bipolar copolyfluorenes in enhancing electroluminescence of MEH−PPV.

Introduction

Since the discovery of the electroluminescence of poly(*p*-phenylenevinylene) (PPV) in 1990,[1] a lot of studies have been focused on polymeric light-emitting diodes (PLEDs) because of their great potential to be applied in large-area and flexible displays.[2] Polymeric materials are attractive due to their good film-forming properties and feasible solution processing techniques via spin-coating and inkjet printing[3−5] and are susceptible to structural modification. However, for most luminescent conjugated polymers such as MEH−PPV, hole injection and transport are more favorable than electron injection and transport due to its high LUMO energy level, resulting in the imbalance of rates for electron and hole injection and lowering the luminance efficiency of the device.[6−10] Balanced and efficient charge injection/transport for both carriers is essential for high device efficiency. To improve the charge injection/transport, two approaches have been attempted. One is to apply an additional electron injection/transport layer between the emitter and cathode and/or a hole transporting layer between the emitter and anode.[11−14] Nevertheless, fabrication of multilayer polymer LEDs is usually a difficult task. From the cost-effective point of view, single-layer devices are preferred. Another approach is to fabricate single-layer LEDs which blend charge injection/transport molecules such as oxadiazole, triazole, triphenylamine, or carbazole derivatives. However, these kinds of small molecules usually have a low glass transition temperature (T_g) that causes crystallization and thermal breakdown during device operation.[15−17] Therefore, the development of charge injection/transport materials with high T_g is very important to enhance device performance. To overcome the above problems, several research groups reported the polymers contain electron- and/or hole-transporting groups with high T_g for improving device performance.[18−23] Greczmiel et al. synthesized polymethacrylates with pendant oxadiazole units for improving device performance.[19] Bellmann et al. synthesized high-T_g hole transporting polymers to improve device performance with a luminance of up to 3700 cd/m^2 and an external quantum efficiency of up to 1.25%.[21a] Jiang et al. synthesized copolymers with hole and electron transport groups to improve single-layer dye-doped device performance with an external quantum efficiency of 0.4%.[21b] Alam et al. synthesized polybenzobisazoles containing electron transport groups to improve the performance of PPV-based devices with a luminance of up to 1400 cd/m^2 and an external quantum efficiency of up to 2.5%.[22a]

Among the typical conjugated polymers, fluorene-based copolymers show good thermal stability[24−26] with high T_g, and the emission spectrum of polyfluorene overlaps partially with the absorption spectrum of MEH−PPV to facilitate energy transfer between them. Aromatic 1,2,4-triazole shows good electron affinity and hole-blocking property, although its solubility in common organic solvents is low.[15,27,28] On the contrary, triphenylamine exhibits good hole affinity and solubility properties.[21a,29] They are two commonly used electron- and hole-transporting moieties in organic and polymeric emitting materials.

In this work, we synthesized a bipolar monomer (**M1**) to prepare copolyfluorenes containing 3.1−11.2 mol % bipolar units. The bipolar unit consists of directly linked electron-transporting aromatic 1,2,4-triazole and hole-transporting triphenylamine. The bipolar copolyfluorenes contain both hole-transporting and electron-affinitive moieties to enhance the injection of holes and electrons. They effectively prevent the π stacking between polymer chains to suppress excimer formation due to nonplanar structure in the bipolar units. Moreover, our results indicate that the copolyfluorenes (**P1**−**P3**) are very effective in promoting emission performance of the conventional MEH−PPV.

Experimental Section

Measurements. ^{1}H NMR spectra were obtained on a Bruker AMX-400 MHz or a AV300 MHz FT-NMR, and chemical shifts were reported in ppm using tetramethylsilane (TMS) as an internal standard. IR spectra were measured as KBr disk on a Fourier transform infrared spectrometer, model 7850 from Jasco. Elemental analysis (EA) was carried out on a Heraus CHN-Rapid elemental analyzer. The M_w and M_w/M_n values of polymers were measured with gel permeation chromatography (GPC) unit using chloroform ($CHCl_3$) as eluent and monodisperse polystyrenes as calibration standards. Thermogravimetric analysis (TGA) of polymers was performed under nitrogen atmosphere at a heating rate of 20 °C /min using a PerkinElmer TGA-7 thermal analyzer. Thermal

* Corresponding author. E-mail: yunchen@mail.ncku.edu.tw.

10.1021/ma9004617 CCC: $40.75
Published on Web 04/20/2009

Scheme 1. Synthesis of Monomer M1 and Model Compound M0

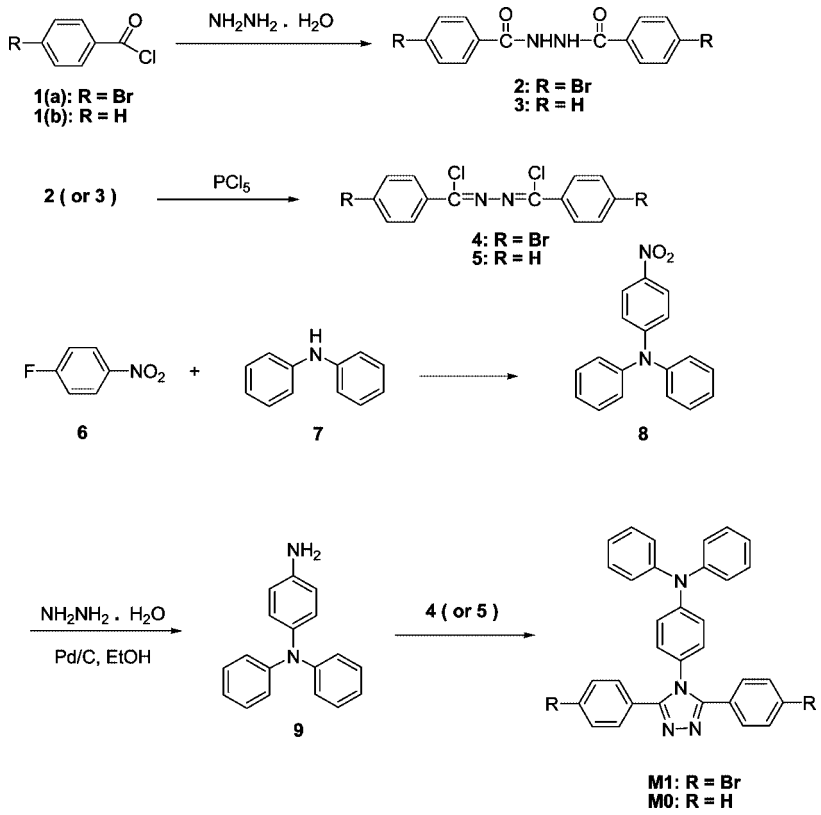

transition properties of polymers were investigated using a differential scanning calorimeter (DSC), PerkinElmer DSC 7, under nitrogen atmosphere at a heating rate of 10 °C/min. Absorption spectra were measured with a Jasco V-550 spectrophotometer, and photoluminescence (PL) spectra were obtained using a Hitachi F-4500 fluorescence spectrophotometer. Cyclic voltammograms were measured with a voltammetric apparatus (model CV-50W from BAS) at room temperature under nitrogen atmosphere. The measuring cell was made up of a polymer-coated glassy carbon as the working electrode, an Ag/AgCl electrode as the reference electrode, and a platinum wire as the auxiliary electrode. The electrodes were supported in acetonitrile containing 0.1 M (n-Bu)$_4$NClO$_4$ as electrolyte. The energy levels were calculated using the value of ferrocene (FOC) (−4.8 eV) with respect to vacuum level, which was defined as zero.[30]

Materials. 9,9-Dihexyl-2,7-dibromofluorene (Aldrich), 9,9-dihexylfluorene-2,7-bis(trimethyleneborate) (Aldrich), Aliquat 336 (Alfa Aesar), tetrakis(triphenylphosphine)palladium [Pd(PPh$_3$)$_4$] (Acros), 4-bromobenzoyl chloride (Acros), phosphorus pentachloride (PCl$_5$, Riedel-Dehaen), *N,N*-dimethylaniline (Acros), dimethyl sulfoxide (DMSO, Tedia), toluene (Tedia), chloroform (CHCl$_3$, Tedia), and other solvents were from commercial sources and used without purification. 1,2-Bis((4-bromophenyl)chloromethylene)hydrazine (**4**) and 1,2-bis(chloro(phenyl)methylene)hydrazine (**5**) were prepared from 4-bromobenzoyl chloride and benzoyl chloride, respectively, by reacting consecutively with hydrazine monohydrate and phosphorus pentachloride (PCl$_5$) (Scheme 1). *N*′,*N*′-Diphenylbenzene-1,4-diamine (**9**) was synthesized from 1-fluoro-4-nitrobenzene (**6**) and diphenylamine (**7**) to obtain *N*-(4-nitrophenyl)-*N*-phenylbenzenamine (**8**), followed by reduction with hydrazine monohydrate. Syntheses of compounds **4**, **5**, and **9** are described in the Supporting Information.

Synthesis of Bipolar Monomer (M1) and Model (M0) (Scheme 1). A mixture of **4** (0.87 g, 2 mmol), **9** (0.52 g, 2 mmol), and 10 mL of *N,N*-dimethylaniline was stirred at 135 °C for 12 h under a nitrogen atmosphere. After adding aqueous solution of HCl (30 mL, 2 N), the mixture was stirred for an additional 30 min. The precipitated solid was collected by filtration, dried in vacuo, and recrystallized from ethyl acetate and chloroform to afford *N*-(4-(3,5-bis(4-bromophenyl)-4*H*-1,2,4-triazol-4-yl)phenyl)-*N*-phenylbenzenamine (**M1**) (54%); mp >250 °C. ^{1}H NMR (CDCl$_3$, ppm): δ 7.51−7.49 (d, J = 8.4 Hz, 4H, Ar−H), 7.40−7.38 (d, J = 8.4 Hz, 4H, Ar−H), 7.35−7.31 (t, J = 8.4 Hz, 4H, Ar−H), 7.15−7.12 (m, 6H, Ar−H), 7.03−7.01 (d, J = 8.8 Hz, 2H, Ar−H), 6.93−6.91 (d, J = 8.8 Hz, 2H Ar−H). FTIR (KBr pellet, cm^{-1}): ν 3070, 2370, 1904, 1592, 1509 (C═N), 1485, 1462, 1333, 1264 (C−N), 1181, 1074 (C−Br), 860. Anal. Calcd (%) for C$_{32}$H$_{22}$Br$_2$N$_4$: C, 61.76; H, 3.56; N, 9.00. Found: C, 61.90; H, 3.63; N, 9.01.

N-Phenyl-*N*-(4-(3,5-diphenyl-4*H*-1,2,4-triazol-4-yl)phenyl)benzenamine) (**M0**), model compound of bipolar unit, was synthesized by analogous procedures used in the preparation of monomer **M1** with a yield of 63%; mp 222−224 °C. ^{1}H NMR (acetone-d_6, ppm): δ 7.55−7.53 (m, 4H, Ar−H), 7.45−7.38 (m, 6H, Ar−H), 7.35−7.31 (t, J = 8.0 Hz, 4H, Ar−H), 7.26−7.24 (d, J = 8.8 Hz, 2H, Ar−H), 7.12−7.10 (m, 6H, Ar−H), 7.05−7.03 (d, J = 8.8 Hz, 2H Ar−H). FTIR (KBr pellet, cm^{-1}): ν 3070, 2537, 1904, 1592, 1509 (C═N), 1485, 1471, 1341, 1272 (C−N), 1181, 1029, 853. Anal. Calcd (%) for C$_{32}$H$_{24}$N$_4$: C, 82.73; H, 5.21; N, 12.06. Found: C, 82.48; H, 5.24; N, 12.05.

Synthesis of Bipolar Copolyfluorenes (P1−P3) and Polyfluorene (PF) (Scheme 2). Copolyfluorenes (**P1−P3**) and poly(9,9-dihexylfluorene) (**PF**) were prepared by palladium-catalyzed Suzuki coupling reaction using (PPh$_3$)$_4$Pd as the catalyst.[31] For instance, stoichiometric amounts of 9,9-dihexylfluorene-2,7-bis(trimethylene borate) (**10**: 0.251 g, 0.50 mmol), 9,9-dihexyl-2,7-dibromofluorene (**11**: 0.222 g, 0.45 mmol), *N*-(4-(3,5-bis(4-bromophenyl)-4*H*-1,2,4-triazol-4-yl)phenyl)-*N*-phenylbenzenamine (**M1**: 0.031 g, 0.05 mmol), 10 mg of (PPh$_3$)$_4$Pd, and several drops of Aliquat 336 were added to a mixture consisting of toluene (10 mL) and 2 M aqueous solution of K$_2$CO$_3$ (8 mL). The solution was refluxed for 48 h under a nitrogen atmosphere. Extra monomer **10** (16 mg, 0.03 mmol) was added to the reaction mixture and stirred for an additional 12 h. Finally, monofunctional bromobenzene (10 mg, 0.07 mmol) was added and stirred for 12 h to end-cap the polymer chain with phenyl

Scheme 2. Synthesis of Bipolar Copolyfluorenes (P1−P3) and Polyfluorene (PF)

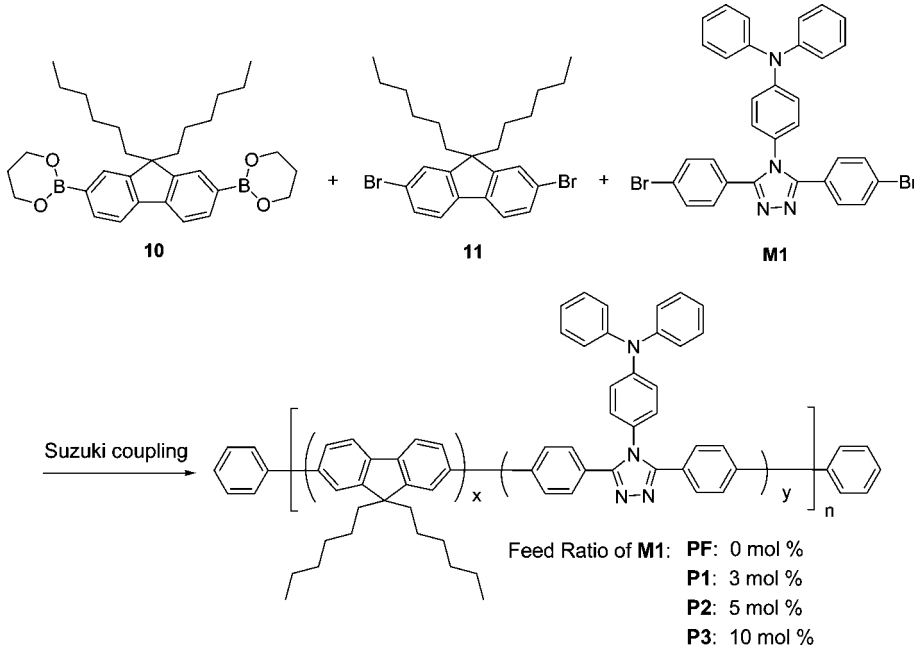

group. After cooling to room temperature, the solution was precipitated from a mixture of methanol and distilled water (v/v = 10/1). The crude polymer precipitate was collected by filtration, dissolved in chloroform, and reprecipitated from methanol twice. Then it was Soxhlet extracted with acetone for 48 h to remove trace oligomers and catalyst residues and dried in vacuo to give **P2**. ^{1}H NMR ($CDCl_3$, ppm): δ 7.85−7.83 (m, 2H, Ar−H), 7.71−7.67 (m, 4H, Ar−H), 7.59 (m, 4H, Ar−H), 7.48 (m, 4H, Ar−H),7.32 (m, 4H, Ar−H), 7.18 (m, 6H Ar−H), 7.16 (m, 2H, Ar−H), 7.11 (m, 2H, Ar−H), 2.12 (s, 4H, $-CH_2-$), 1.25 (s, 4H, $-CH_2-$), 1.13 (s, 12H, $-CH_2-$), 0.79 (s, 6H, $-CH_3$). FTIR (KBr pellet, cm^{-1}): ν 3032, 2926 (Ar−H), 2857, 1889, 1592, 1509 (C═N), 1455 (C═C), 1280 (C−N), 1112, 998, 891. Anal. Calcd (%) for **P2**: C, 89.76; H, 9.41; N, 0.83. Found: C, 88.49; H, 9.51; N, 0.59.

The synthetic procedures of **PF**, **P1**, and **P3** were similar to those used in the preparation of **P2**, except with varied molar feed ratios in **10**, **11**, and **M1**. **PF**: **10** (0.251 g, 0.50 mmol), **11** (0.246 g, 0.50 mmol). ^{1}H NMR ($CDCl_3$, ppm): δ 7.85−7.83 (m, 2H, Ar−H), 7.71−7.67 (m, 4H, Ar−H), 2.12 (s, 4H, $-CH_2-$), 1.25 (s, 4H, $-CH_2-$), 1.13 (s, 12H, $-CH_2-$), 0.84−0.78 (m, 6H, $-CH_3$). FTIR (KBr pellet, cm^{-1}): ν 3032, 2926 (Ar−H), 2849, 2370, 1889, 1607, 1455 (C═C), 1409, 1371, 1250, 1089, 884. Anal. Calcd (%) for **PF**: C, 90.26; H, 9.74. Found: C, 88.37; H, 9.43. **P1**: **10** (0.251 g, 0.50 mmol), **11** (0.231 g, 0.47 mmol) and **M1** (0.018 g, 0.03 mmol). ^{1}H NMR ($CDCl_3$, ppm): δ 7.85−7.83 (m, 2H, Ar−H), 7.71−7.67 (m, 4H, Ar−H), 7.52−7.47 (m, 4H, Ar−H), 7.37−7.36 (m, 4H, Ar−H), 7.14 (m, 10H, Ar−H), 2.17−2.12 (m, 4H, $-CH_2-$), 1.25 (s, 4H, $-CH_2-$), 1.13 (s, 12H, $-CH_2-$), 0.83−0.78 (s, 6H, $-CH_3$). FTIR (KBr pellet, cm^{-1}): ν 3032, 2926 (Ar−H), 2852, 1889, 1606, 1509 (C═N), 1455 (C═C), 1280 (C−N), 1114, 998, 891. Anal. Calcd (%) for **P1**: C, 89.96; H, 9.54; N, 0.50. Found: C, 88.73; H, 9.34; N, 0.38. **P3**: **10** (0.251 g, 0.50 mmol), **11** (0.197 g, 0.40 mmol) and **M1** (0.062 g, 0.10 mmol). ^{1}H NMR ($CDCl_3$, ppm): δ 7.83 (m, 2H, Ar−H), 7.67 (m, 4H, Ar−H), 7.50 (m, 4H, Ar−H), 7.32 (m, 4H, Ar−H), 7.19 (m, 6H, Ar−H), 7.16 (m, 2H, Ar−H), 7.11 (m, 2H, Ar−H), 2.12 (s, 4H, $-CH_2-$), 1.25 (s, 4H, $-CH_2-$), 1.13 (s, 12H, $-CH_2-$), 0.79 (s, 6H, $-CH_3$). FTIR (KBr pellet, cm^{-1}): ν 3032, 2926 (Ar−H), 2857, 1889, 1592, 1509 (C═N), 1455 (C═C), 1280 (C−N), 1112, 998, 891. Anal. Calcd (%) for **P3**: C, 89.28; H, 9.09; N, 1.63. Found: C, 87.55; H, 8.96; N, 1.36.

Fabrication of Electroluminescent Devices. Double-layer polymer light-emitting diodes (PLEDs) with a configuration of ITO/PEDOT:PSS/polymer/Ca/Al were fabricated to investigate their electroluminescent characteristics. Transparent indium tin oxide (ITO) glass was subsequently cleaned with neutraler reiniger/deionized water (1:3 volume) mixture, deionized water, acetone, and 2-propanol, and then dried in vacuo overnight. Aqueous dispersion of PEDOT:PSS was spin-coated on top of the cleaned ITO glass as hole-injection layer and dried at 150 °C for 15 min. Emitting layer was then formed by spin-coating (1000 rpm) onto the PEDOT:PSS layer from a polymer solution in 1,2-dichlorobenzene (10 mg/mL). Finally, calcium and aluminum were consecutively vacuum-deposited as cathode using a vacuum coater at a pressure of 2×10^{-6} Torr. Luminance and current density vs voltage characteristics of the devices were measured with a power supply (Keithley 2400), and EL spectra were recorded with a fluorescence spectrophotometer (Ocean Optics usb2000). The optoelectronic measurements were conducted in a glovebox filled with nitrogen.

Results and Discussion

1. Characterization of Bipolar Monomer (M1) and Copolyfluorenes (P1−P3). Scheme 1 illustrates the synthetic routes used in the preparation of bipolar model compound **M0** and main monomer **M1**. 1,2-Bis((4-bromophenyl)chloromethylene)hydrazine (**4**)[28b] and *N*-(4-nitrophenyl)-*N*-phenylbenzenamine (**8**)[32] were prepared according to the procedures reported previously. The copolyfluorenes (**P1−P3**) were synthesized by the Suzuki coupling reaction between 9,9-dihexylfluorene-2,7-bis(trimethyleneborate) (**10**) and functionalized dibromo aromatic monomers (**11** and **M1**) (Scheme 2), using $Pd(PPh_3)_4$ as reaction catalyst and Aliquat 336 as phase-transfer catalyst. The feed ratios of monomer **M1** in the preparation of **P1**, **P2**, and **P3** were 3, 5, and 10 mol %, respectively. Extra monomer **10** and monofunctional bromobenzene were added to end-cap polymer chain end after the polymerization. Figure S1 (Supporting Information) shows the ^{1}H NMR, ^{13}C NMR, DEPT135, H−H COSY, and C−H HMQC spectra of **M1**. Assignments of each carbon and proton are assisted by the two-dimensional NMR spectra (Figure S1d,e), which agree with the proposed molecular structure of **M1**. The main ^{1}H NMR spectral difference between **PF** and **P3** lies in chemical shift regions at 7.32−7.26 and 7.19−7.11 ppm which originate from incorporated **M1** residues (Figure S2a). The existence of **M1** residue in **P3** is confirmed by ^{13}C NMR and DEPT135 spectra of **M1**, **PF**, and **P3** as shown in Figure S1b,c and Figure S2b,c. In ^{13}C

Table 1. Polymerization Results and Characterization of Polymers

polymer	yield (%)	M_n[a] ($\times 10^3$)	M_w[a] ($\times 10^4$)	PDI[a]	T_g (°C)	T_d[b] (°C)	y[c] (%)
PF	63	9.45	2.42	2.54	91	428	0
P1	64	8.02	1.60	1.99	94	440	3.1
P2	53	8.10	1.76	2.16	104	449	4.8
P3	54	8.55	1.78	2.08	112	450	11.2

[a] M_n, M_w, and PDI of the polymers were determined by gel permeation chromatography using polystyrene standards. [b] The temperature at 5 wt % loss under a nitrogen atmosphere. [c] The molar fractions of **M1** residues were estimated from elemental analysis (EA).

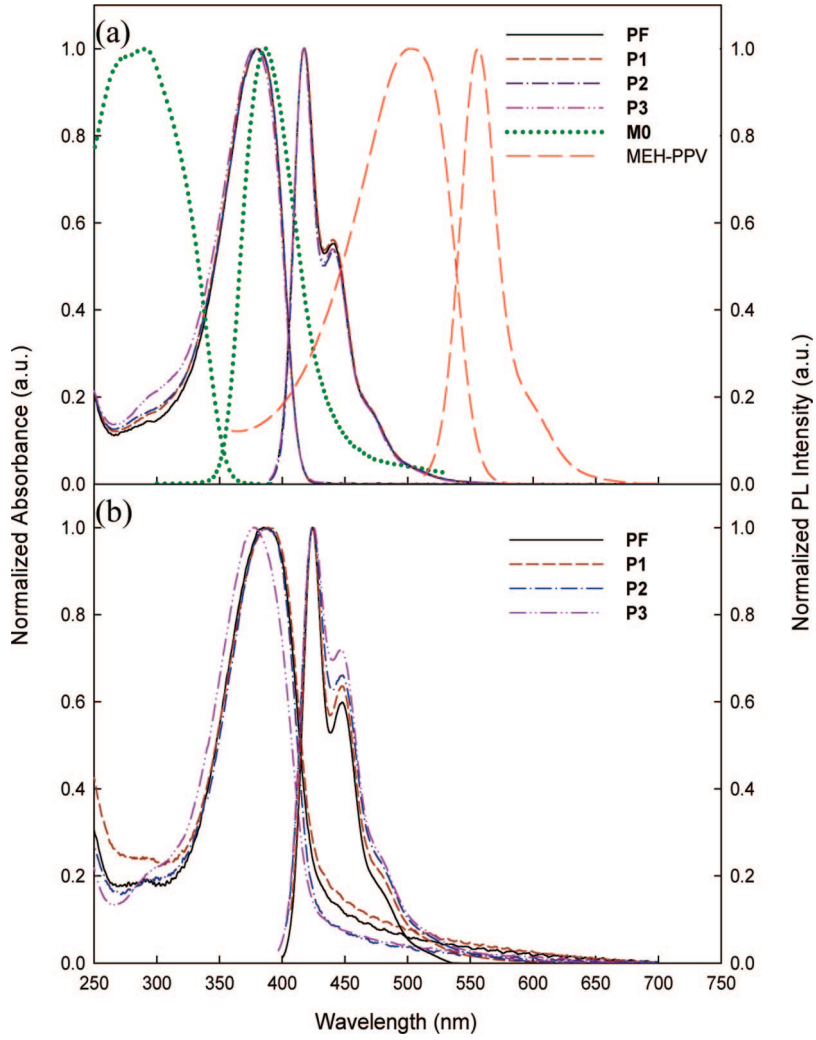

Figure 1. Absorption and PL spectra of **M0**, **PF**, and **P1**−**P3**: (a) in chloroform (1×10^{-5} M) (λ_{ex} = 292 nm for **M0**, 378 nm for **P3**, and 380 nm for **PF**, **P1**, **P2**); (b) in film state (λ_{ex} = 378 nm for **P3** and 387 nm for **PF**, **P1**, **P2**).

NMR spectra of **P3** chemical shifts of **M1** residue are obviously observed at 154.8 ppm (8), 146.7 ppm (10), and 149.2 ppm (11). The molar percents of **M1** residues in **P1**, **P2**, and **P3** are 3.1, 4.8, and 11.2 mol % estimated from element analysis data. The copolyfluorenes are soluble in common organic solvents such as toluene, chloroform, chlorobenzene, and 1,2-dichlorobenzene. Their weight-average molecular weights (M_w) and polydispersity indexes (PDI) are (1.60−2.42) $\times$ 10^4 and 1.99−2.54 (Table 1), respectively, as determined by gel permeation chromatography using polystyrenes as calibration standards.

Thermal resistance and thermal transition properties of **PF** and **P1**−**P3** were investigated with thermogravimetric analysis (TGA) and differential scanning calorimetry (DSC). The copolyfluorenes reveal higher thermal decomposition temperatures (440−450 °C) than **PF** (428 °C), with residual weights (at 800 °C) above 50% under a nitrogen atmosphere (Supporting Information). The glass-transition temperatures (T_g), determined from the second heating DSC scans, are 91 °C for **PF**, 94 °C for **P1**, 104 °C for **P2**, and 112 °C for **P3**. Clearly, incorporation of **M1** into **PF** main chain renders a gradual increase in the glass transition temperature. This is attributable to rigid aromatic 1,2,4-triazole units which not only enhance chain rigidity but also reduce chain mobility of polyfluorene.[33] Accordingly, the copolyfluorenes exhibit better thermal stability than **PF**; i.e., their glass transition (94−112 °C) and thermal decomposition temperatures (440−450 °C) are higher than those of **PF** (91 °C, 428 °C).

2. Photophysical Properties of Bipolar Copolyfluorenes. The absorption and photoluminescence (PL) spectra of model **M0**, **PF**, and **P1**−**P3** in $CHCl_3$ and as films spin-coated from $CHCl_3$ solutions are shown in Figure 1, with the corresponding optical data summarized in Table 2. The **M0** in solution shows an absorption maximum at ca. 292 nm (with a shoulder at 271 nm) and a main emission peak at 386 nm. The absorption maxima of **P1**−**P3** in $CHCl_3$ are very close and situate at 378−380 nm, with small shorter wavelength absorptions at ca.

Table 2. Optical Properties of Model M0 and Polymers

molecule/ polymer	UV−vis λ_{max} (nm)		PL λ_{max}		Φ_{PL}[c]
	solution[a]	film	solution[b] (nm)	film[b] (nm)	
M0	271, 292		386		
PF	380	387	418, 440	425, 447	0.79
P1	292, 380	293, 387	418, 440 s	425, 447 s	0.75
P2	292, 380	293, 387	417, 440 s	424, 447 s	0.77
P3	292, 378	292, 378	417, 440 s	424, 447 s	0.72

[a] In chloroform (1×10^{-5} M). [b] s: wavelength of shoulder. [c] Φ_{PL}: determined in $CHCl_3$, relative to quinine sulfate in 1 N $H_2SO_{4(aq)}$ at a concentration of 10^{-5} M ($\Phi_{PL} = 0.55$).

292 nm. The major absorption of **P1**−**P3** (378−380 nm) can be attributed to the $\pi-\pi^*$ transitions of their conjugated backbone, whereas the shorter-wavelength absorption (ca. 292 nm) is ascribed to the absorption of incorporated **M1** residues. The absorption maxima of **P1** and **P2** in film state are red-shifted about 7 nm relative to those in solution due to aggregate formed via intra- or interchain interaction. However, the absorption of **P3** reveals no obvious red shift under the same state transformation. Therefore, the aggregate formation can be effectively suppressed at high content of nonplanar of **M1** residues (11.2 mol %). The PL spectra of **P1**−**P3** locate at 417−418 nm and are almost identical to the emission band of **PF** (λ_{max}= 418 nm). Moreover, the PL spectra of **P1**−**P3** are almost identical to that of **PF** whether they are excited with 292 nm (absorption maximum of **M0**) or 380 nm, suggesting efficient energy transfer from **M1** residues to fluorene segments under the photoexcitation. Partial spectral overlap between emission spectrum of **M1** residues and absorption spectrum of **PF** contributes greatly to the Förster energy transfer.[33,34] It is noteworthy that emission spectrum of **PF** also partially overlaps with absorption spectrum of MEH−PPV (Figure 1a), suggesting that energy transfer from **PF** to MEH−PPV can be expected. On the basis of this characteristic, we fabricated efficient EL devices using blends of MEH−PPV and **P1**−**P3** as emitting layer and will be discussed later.

Relative PL quantum yields (Φ_{PL}) of **PF**, **P1**, **P2**, and **P3** are 0.79, 0.75, 0.77, and 0.72, respectively, in which the Φ_{PL}s of the copolyfluorenes are slightly lower than that of **PF**, probably caused by torsion-induced nonradiative deactivation occurred at nonplanar **M1** residues.[35] Undesirable green emission usually appears during thermal annealing or device operation for **PF**, which has been attributed to enhanced intermolecular interaction.[36] Color stability of the polymers against heat treatment was examined by annealing at 150 °C in vacuum for 24 h. An emission appears at ca. 500−600 nm in the PL spectrum of **PF** film after thermal annealing (Figure 2); however, the green emission is significantly suppressed in **P1**−**P3** films under the same treatment. This result suggests that the nonplanar structure of **M1** residues in the copolyfluornes is effective in suppressing the formation of intermolecular interaction.

3. Electrochemical Investigations. Cyclic voltammetry (CV) was employed to investigate the reduction−oxidation behaviors of model **M0**, **PF**, and **P1**−**P3**. Their HOMO and LUMO energy levels were estimated by the equations E_{HOMO} (eV) = $-(E_{onset(ox),FOC} + 4.8)$ and E_{LUMO} (eV) = $-(E_{onset(red),FOC} + 4.8)$, where $E_{onset(ox),FOC}$ and $E_{onset(red),FOC}$ are the onset oxidation and onset reduction potentials, respectively, relative to ferrocene/ferrocenium couple. The cyclic voltammograms are shown in Figure 3, and their electrochemical data are summarized in Table 3. Electrochemically estimated band gaps (E_g^{el}), calculated using E_g^{el} = LUMO − HUMO, are different from optical band gaps (E_g^{opt}) obtained from onset absorption.[23c,28b] The discrepancy is especially significant for **P3** (0.17 eV). The electrochemical band gaps (E_g^{el}) are the difference between the LUMO and HOMO levels, which are estimated from onset oxidation and reduction potentials, respectively. Oxidation and reduction of a

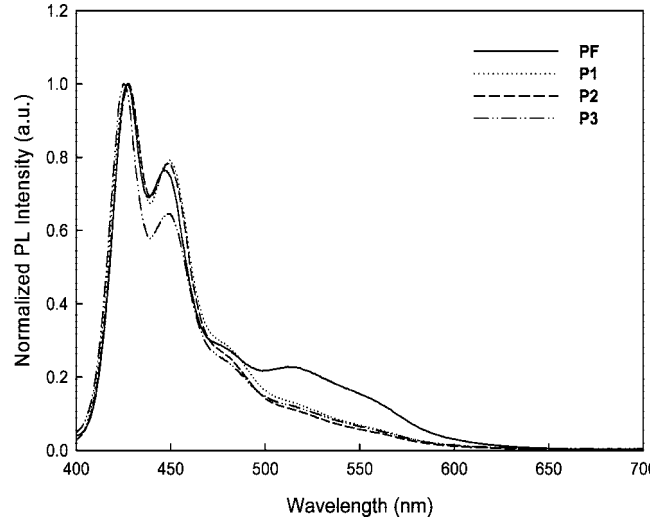

Figure 2. PL spectra of **PF** and **P1**−**P3** after annealing in vacuum at 150 °C for 24 h.

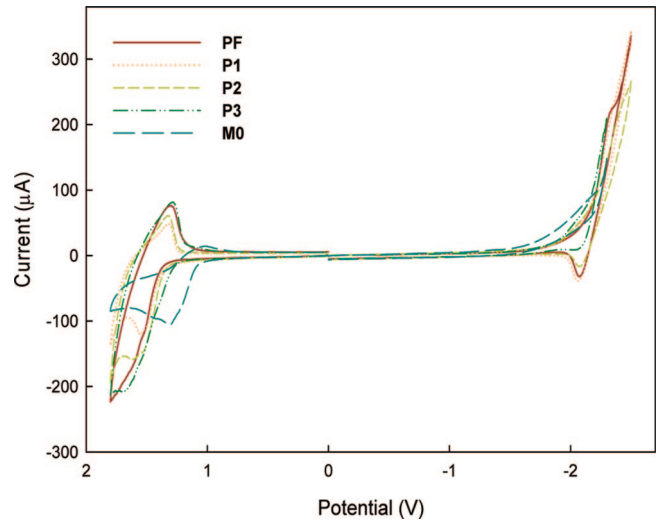

Figure 3. Cyclic voltammograms of **M0**, **PF**, and **P1**−**P3** coated on glassy carbon working electrode (scan rate: 100 mV/s).

polymer may start from different parts if it contains electron-donating and electron-withdrawing groups simultaneously. For example, the oxidation of **P3** starts from triphenylamine units, while the reduction begins at triazole moieties. However, the optical band gaps (E_g^{opt}) are estimated from the longer onset wavelength of absorption spectra. As a result of different estimation bases, large discrepancy between electrochemical and optical band gaps is usually obtained in bipolar copolymers, such as **P3**. In this study, copolyfluorenes **P1**−**P3** contain 3.1−11.2 mol % of bipolar **M1** residues derived from electron-transporting triazole and hole-transporting triphenylamine. The HOMO energy levels of **M0**, **PF**, and **P1**−**P3** are −5.3, −5.63, −5.62, −5.59, and −5.49 eV, whereas the LUMO energy levels are −2.77, −2.54, −2.63, −2.65, and −2.68 eV, respectively. The HOMO levels of **P1**−**P3** are raised gradually from −5.62 to −5.49 eV with an increase in **M1** residues (3.1−11.2 mol %) (Figure 4), suggesting that their hole affinity is in the order of **P3** > **P2** > **P1**. On the contrary, the LUMO levels of **P1**−**P3** are lowered slightly (−2.63 to −2.68 eV) with increasing **M1** residues, meaning that their electron injection ability is improved in the order of **P3** > **P2** > **P1**. Therefore, both hole and electron affinity of **P1**−**P3** are gradually enhanced with increasing **M1** residues, resulting in improvement in hole and electron injection. Both LUMO and HOMO energy levels of **M0** (−2.77 and −5.3

Table 3. Electrochemical Properties of Model M0 and Polymers (PF, P1−P3)

molecule/polymer	$E_{onset(ox)}$ vs FOC (V)[a]	$E_{onset(red)}$ vs FOC (V)[a]	E_{HOMO} (eV)[b]	E_{LUMO} (eV)[b]	E_g^{el} (eV)[c]	E_g^{opt} (eV)[d]
M0	0.5	−2.03	−5.3	−2.77	2.53	
PF	0.83	−2.26	−5.63	−2.54	3.09	3.00
P1	0.82	−2.17	−5.62	−2.63	2.99	3.00
P2	0.81	−2.15	−5.59	−2.65	2.94	2.99
P3	0.69	−2.14	−5.49	−2.68	2.81	2.98

[a] E_{FOC} = 0.48 V vs Ag/AgCl. [b] $E_{HOMO} = -e(E_{onset(ox),\ FOC} + 4.8\ V)$; $E_{LUMO} = -e(E_{onset(red),\ FOC} + 4.8\ V)$. [c] Electrochemical band gap: E_g^{el} = LUMO − HOMO. [d] Optical band gap: $E_g^{opt} = hc/\lambda_{onset}$.

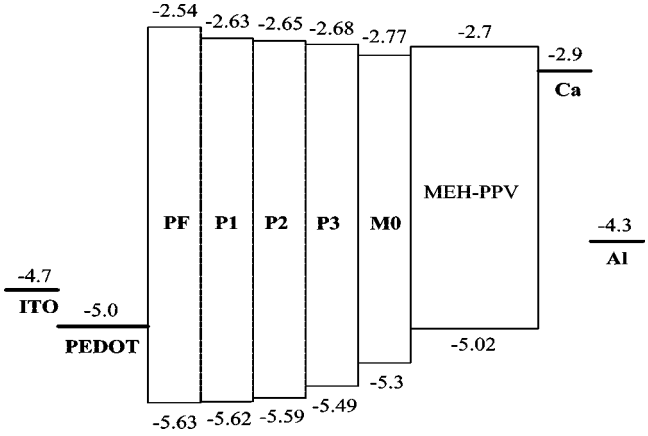

Figure 4. Energy band diagrams of **M0**, **PF**, **P1**−**P3**, and MEH−PPV.

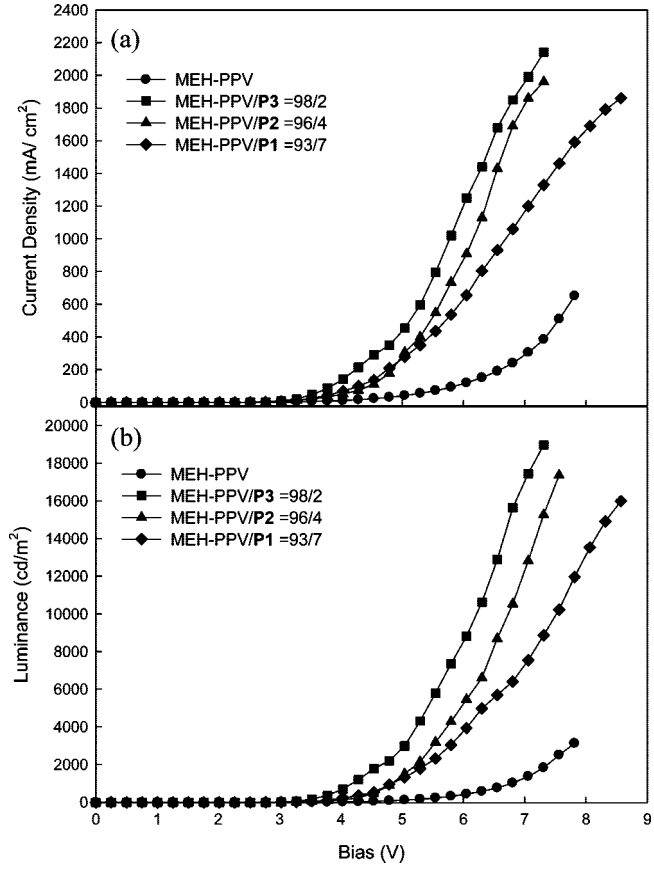

Figure 5. (a) Current density-bias characteristics and (b) luminance-bias characteristics of EL devices using blends of MEH−PPV and **P1**−**P3** (2−7 wt %) as emitting layer. Device configuration: ITO/PEDOT:PSS/MEH−PPV + **P1**, **P2**, or **P3**(90−110 nm)/Ca(50 nm)/Al(100 nm).

eV) are lower than those of MEH−PPV (−2.7 and −5.02 eV) because of the electron-withdrawing aromatic 1,2,4-triazole moiety and electron-donating triphenylamine groups, respectively.[23c] Therefore, blending **P1**−**P3** with the conventional MEH−PPV would increase its electron affinity and at the same time reduce its hole affinity. This might be an effective way in improving balance in charge injection/transport in conventional MEH−PPV whose hole injection and transport are believed to be much better than electron.

4. Electroluminescent Enhancement of MEH−PPV by Bipolar Copolyfluorenes. Electroluminescent devices with **P1**−**P3** as emitting layers [ITO/PEDOT:PSS/**P1**−**P3**/Ca(50 nm)/Al(100 nm)] were fabricated to study their emitting characteristics. The turn-on voltages of **P1**−**P3** devices increased from 5.2 to 9.3 V with increasing **M1** residues (3.1−11.2%). The maximum luminance and maximum luminance efficiency of **P1**−**P3** devices decrease from 1050 to 380 cd/m^2 and from 0.29 to 0.14 cd/A, respectively, with increasing **M1** residues (from 3.1 to 11.2 mol %). The performance degradation at high content of **M1** residues is probably due to charge trapping in the bipolar moieties that reduce charge recombination in polyfluorene segments.[37,38] According to the energy band diagrams depicted in Figure 4, however, both LUMO and HOMO levels of model **M0** are lower than those of MEH−PPV, suggesting that the bipolar units will promote electron injection and block hole transport in the MEH−PPV device. Accordingly, we blended **P1**−**P3** with MEH−PPV to improve the common defect of charge imbalance of the latter. Double-layer electroluminescent devices using blends of **P1**−**P3** and MEH−PPV as emitting layers [ITO/PEDOT:PSS/(MEH−PPV + **P1**, **P2**, or **P3**)/Ca(50 nm)/Al (100 nm)] were fabricated and their device performances investigated. The weight ratios of MEH−PPV to the copolyfluorenes (MEH−PPV/**P1**, MEH−PPV/**P2**, and MEH−PPV/**P3**) are adjusted at 93/7, 96/4, and 98/2 wt %, respectively, to make the contents of bipolar **M1** residues in the blends roughly the same. The current density and luminance versus bias characteristics of the blend devices are shown in Figure 5, with the corresponding performance data summarized in Table 4. Turn-on voltages of the blending systems (2.9−3.2 V) are lower than that of MEH−PPV device (3.8 V) (Table 4). The maximum luminance and maximum luminance efficiency of the blend devices are improved to 18 970 cd/m^2 and 0.89 cd/A, respectively, from 3120 cd/m^2 and 0.49 cd/A of the device using neat MEH−PPV as emitting layer. This is attributable to more balanced electron- and hole-injection/transport in the blend devices due to the presence of bipolar **M1** residues. The performance of blend device from **P3** is superior to those from **P1** and **P2**, probably due to the least polyfluorene contents (ca. 1.8 wt %) in the emitting layer. This is the first report on significant enhancement of EL device performance through blending a small quantity (ca. 0.2 wt %) of bipolar groups.

We also attempted to investigate the influence of bipolar content on device performance, using blends of **P3** and MEH−PPV as emitting layer. The current density and luminance versus bias of the MEH−PPV/**P3** devices are shown in Figure 6. The turn-on voltages of the device (2.9−3.7 V) are lower than that of MEH−PPV device (3.8 V) due to improved electron-injection/transport. However, the turn-on voltages increase gradually from 2.9 to 3.7 V with increasing **P3** contents (2−20 wt %). Accordingly, the enhancement in electron

Table 4. Optoelectronic Performance of Electroluminescent Devices[a]

emitting-layer composition[b]	turn-on voltage (V)[c]	max luminance efficiency (cd/A)	max luminance (cd/m^2)	CIE coordinates (x, y)[d]
MEH−PPV	3.8	0.49	3120	(0.58, 0.42)
MEH−PPV/**PF** (95.5/4.5)	3.2	0.21	2220	(0.56, 0.43)
MEH−PPV/**P1** (93/7)	3.2	0.86	15980	(0.52, 0.48)
MEH−PPV/**P2** (96/4)	3.2	0.81	17370	(0.52, 0.48)
MEH−PPV/**P3** (98/2)	2.9	0.89	18970	(0.50, 0.50)
MEH−PPV/**P3** (95/5)	3.3	1.08	19560	(0.53, 0.47)
MEH−PPV/**P3** (92/8)	3.4	0.54	7200	(0.56, 0.44)
MEH−PPV/**P3** (87.5/12.5)	3.5	0.54	3910	(0.57, 0.43)
MEH−PPV/**P3** (80/20)	3.7	0.38	2830	(0.55, 0.45)

[a] Device structure: ITO/PEDOT:PSS/emitting-layer/Ca/Al. [b] The weight ratios are given in parentheses. [c] The voltage required for the luminance of 10 cd/m^2. [d] The CIE coordinates at maximum luminance.

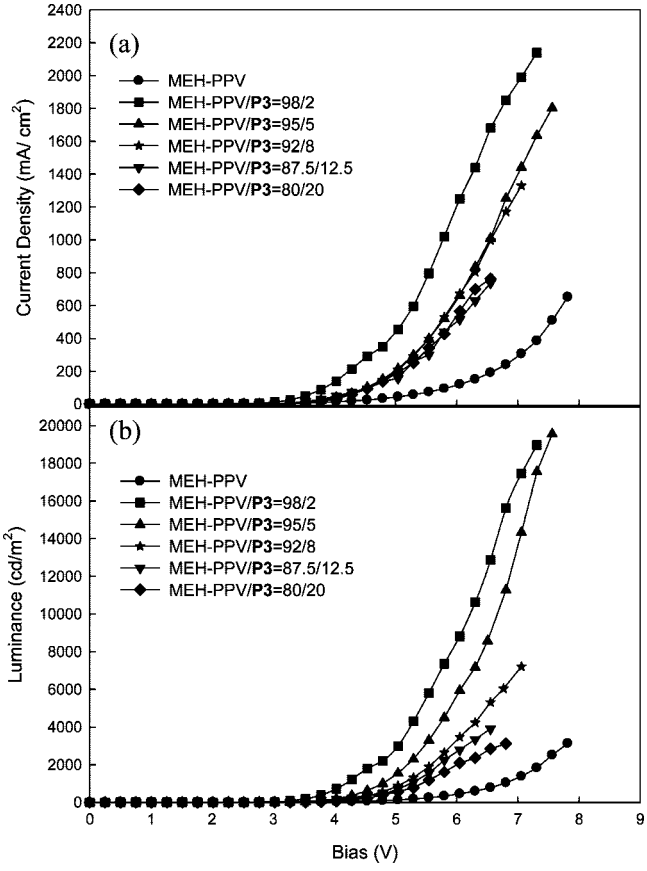

Figure 6. (a) Current density−bias characteristics and (b) luminance−bias characteristics of EL devices using blends of MEH−PPV and **P3** (2−20 wt %) as emitting layer. Device structure: ITO/PEDOT:PSS/MEH−PPV + **P3** (90−110 nm)/Ca(50 nm)/Al(100 nm).

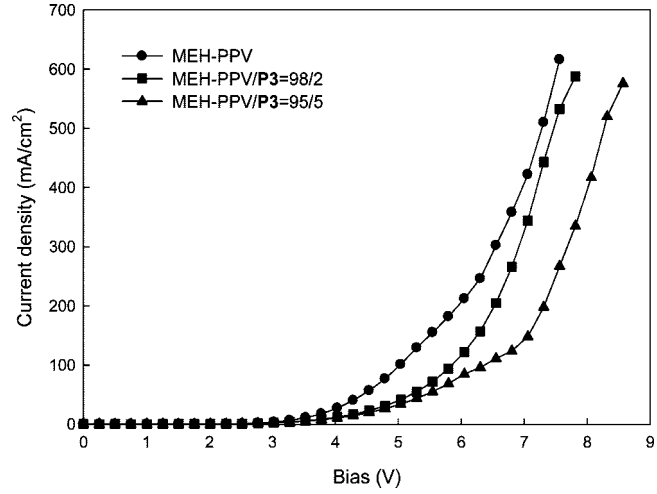

Figure 7. Current density-bias characteristics of the hole-only devices using blends of MEH−PPV and **P3** (0−5 wt %) as emitting layer. Device structure: ITO/PEDOT:PSS/MEH−PPV + **P3**(90−110 nm)/Au(20 nm)/Al(100 nm).

injection is inferior to hole-blocking effect that needs extra bias to turn on the devices.[39] In order to elucidate the hole-blocking effect of **P3** in blend devices, hole-only devices were fabricated [ITO/PEDOT:PSS/(MEH−PPV+ **P3**)/Au(20 nm)/Al (100 nm)] and their current density-bias characteristics investigated. As shown in Figure 7, the curve shifts horizontally to higher bias with increasing **P3** contents. At a bias of 6 V, the current density decreases from 210 to 85 mA/cm^2 with an increase in **P3** contents (from 0 to 5 wt %). Clearly, the current density decrease is mainly attributed to the hole-blocking effect of the bipolar units. EL device using blend of MEH−PPV and **PF** as emitting layer was also fabricated to compare with those obtained from copolyfluorenes (MEH−PPV/**P1**−**P3**) to elucidate the contribution of the bipolar units. Its maximum luminance efficiency (0.21 cd/A) and maximum luminance (2220 cd/m^2) are lower than those of the MEH−PPV device (0.49 cd/A, 3120 cd/m^2), as shown in Table 4. This clearly indicates that the performance enhancement in copolymer blend devices (MEH−PPV/**P1**−**P3**) is mainly attributed to the bipolar **M1** residues. The maximum luminance of the device is enhanced from 3120 to 19 560 cd/m^2, and the maximum luminance efficiency is also improved from 0.49 to 1.08 cd/A as the weight ratio of **P3** is increased from 0 to 5%. However, further increase in **P3** contents leads to quick degradation in maximum luminance and maximum luminance efficiency, i.e., diminish to 2830 cd/m^2 and 0.38 cd/A at MEH−PPV/**P3** = 80/20, respectively. It is noteworthy that the EL efficiency of the blend devices depends upon the content of both bipolar units and fluorene segments. As mentioned above, the blend device obtained from MEH−PPV/**P3** (98/2) shows higher luminance efficiency (0.89 cd/A) than those from MEH−PPV/**P1** (93/7) and MEH−PPV/**P2** (96/4) due to its lower content of fluorene segments, although their contents of the bipolar units are almost the same. In addition, the luminance efficiency of MEH−PPV/**P3** devices is enhanced significantly (from 0.49 to 1.08 cd/A) when the weight ratio of **P3** is increased from 0 to 5%. This indicates that the EL efficiency of the blend devices exhibits enhancing tendency with an increase in content of the bipolar units. Therefore, the inferior performance at high **P3** composition is not caused by the greater concentration of the bipolar units. The result of morphology investigation can reasonably explain this performance reversion at higher **P3** contents. As shown in Figure 8, at low ratio of **P3** (MEH−PPV/**P3** = 95/5) the SEM micrograph shows a homogeneous surface morphology. However, the morphology becomes obviously microphase separated at high **P3** ratio (MEH−PPV/**P3** = 80/20). Therefore, the quick degradation of device performance can be attributed to the microphase separation formed during film preparation. However, our results show that low concentration of the bipolar units is already effective in enhancing optoelectronic performance of the conventional MEH−PPV. The 1931 CIE chro-

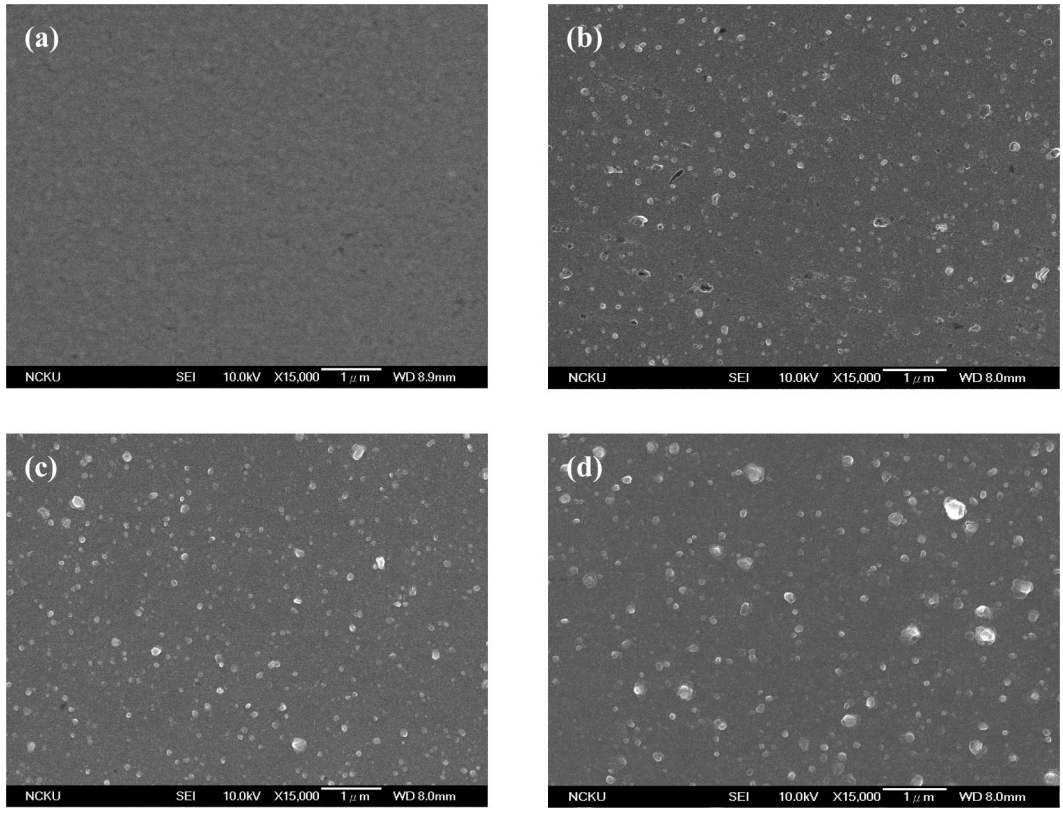

Figure 8. SEM micrographs of blend films: (a) MEH−PPV/**P3** = 95/5, (b) MEH−PPV/**P3** = 92/8, (c) MEH−PPV/**P3** = 87.5/12.5, and (d) MEH−PPV/**P3** = 80/20.

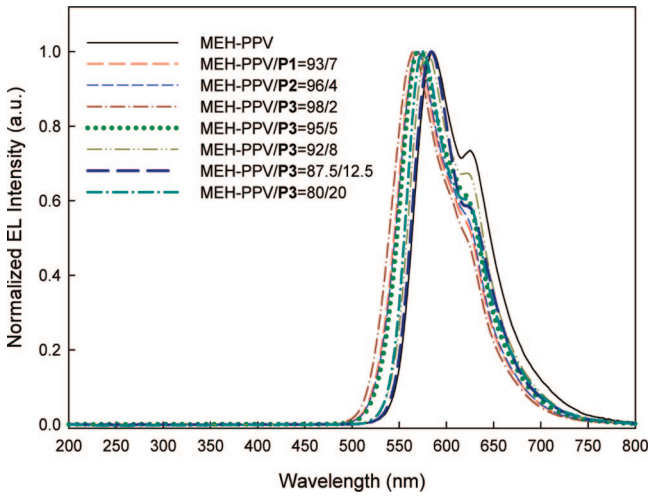

Figure 9. EL spectra of devices using blends of MEH−PPV and **P1**−**P3** as emitting layer. Device configuration: ITO/PEDOT:PSS/MEH−PPV + **P1**, **P2**, or **P3** (90−110 nm)/Ca(50 nm)/Al(100 nm).

maticity coordinates of the EL emission shift slightly from (0.58, 0.42) of the pure MEH−PPV device to (0.50, 0.50) of blend device (MEH−PPV/**P3** = 98/2) (Table 4). The emission is mainly originated from MEH−PPV (500−750 nm) for all devices, and their full widths at half-maximum (fwhm) are almost the same (ca. 90 nm) (Figure 9). However, the EL emissions of the blend devices reveal slight blue shift (14−20 nm) and diminished emission at ca. 630 nm (excimer emission of MEH−PPV), which is probably due to reduced aggregation after blending with the copolyfluorenes.

Conclusion

We successfully synthesized copolyfluorenes (**P1**−**P3**) containing bipolar *N*-phenyl-*N*-(4-(3,5-diphenyl-4*H*-1,2,4-triazol-4-yl)phenyl)benzenamine (**M0**: 3.1, 4.8, and 11.2 mol %). The copolymers were soluble in common organic solvents and thermally stable (thermal decomposition temperature: 428−450 °C). The PL spectra of **P1**−**P3** (λ_{ex} = 292 nm) were identical to that of **PF** (λ_{ex} = 380 nm) due to efficient Förster energy transfer. The interchain interaction commonly occurred in **PF** was effectively suppressed after incorporating the bipolar moieties. The HOMO and LUMO levels of model **M0** were −5.3 and −2.77 eV, respectively. The HOMO levels of **PF** and **P1**−**P3** were raised gradually from −5.63 to −5.49 eV with increasing bipolar units (from 0 to 11.2 mol %), while their LUMO levels lowered from −2.54 to −2.68 eV. Blending the copolyfluorenes with conventional MEH−PPV significantly enhanced its device performance due to improved carrier injection. The EL device using blend of MEH−PPV and **P3** (MEH−PPV/**P3** = 95/5) as emitting layer showed the best performance (maximum luminance: 19 560 cd/m^2; maximum luminance efficiency: 1.08 cd/A), which were superior to those using MEH−PPV as emitting layer. Current results indicate that the copolyfluorenes containing bipolar moieties are very promising additive in promoting electroluminescent performance of MEH−PPV and other conjugated polymers.

Acknowledgment. We thank the National Science Council of the Republic of China for financial aid through Project NSC 95-2221-E006-226-MY3.

Supporting Information Available: Experimental details and characterization of monomers (**2**−**5**, **8**, **9**), ^{1}H NMR and ^{13}C NMR spectra of **M1**, **PF**, and **P3**, TGA thermograms and DSC traces of **PF** and **P1**−**P3**, absorption and PL spectra of blends in solution or

film state. This material is available free of charge via the Internet at http://pubs.acs.org.

References and Notes

(1) Burroughes, J. H.; Bradley, D. D. C.; Brown, A. R.; Marks, R. N.; Mackay, K.; Friend, R. H.; Burn, P. L.; Holmes, A. B. *Nature (London)* **1990**, *347*, 539.

(2) (a) Grem, G.; Leditzky, G.; Ullrich, B.; Leising, G. *Adv. Mater.* **1992**, *4*, 36. (b) Pei, Q.; Yang, Y. *J. Am. Chem. Soc.* **1996**, *118*, 7416. (c) Andersson, M. R.; Thomas, O.; Mammo, W.; Svensson, M.; Theander, M.; Inganäs, O. *J. Mater. Chem.* **1999**, *9*, 1933.

(3) Kraft, A.; Grimsdale, A. C.; Holmes, A. B. *Angew. Chem., Int. Ed.* **1998**, *37*, 402.

(4) Friend, R. H.; Gymer, R. W.; Holmes, A. B.; Burroughes, J. H.; Marks, R. N.; Taliani, C.; Bradley, D. D. C.; Dos Santos, D. A.; Brédas, J. L.; Lögdlund, M.; Salaneck, W. R. *Nature (London)* **1999**, *397*, 121.

(5) (a) Bernius, M. T.; Inbasekaran, M.; O'Brien, J.; Wu, W. *Adv. Mater.* **2000**, *12*, 1737. (b) Akcelrud, L. *Prog. Polym. Sci.* **2003**, *28*, 875.

(6) (a) Takiguchi, T.; Park, D. H.; Yoshino, K. *Synth. Met.* **1987**, *17*, 657. (b) Braun, D.; Heeger, A. J. *Appl. Phys. Lett.* **1991**, *58*, 1982.

(7) (a) Kraft, A.; Burn, P. L.; Holmes, A. B.; Bradley, D. D. C.; Friend, R. H.; Martens, J. H. F. *Synth. Met.* **1993**, *72*, 4163. (b) Antomiadis, H.; Abkowitz, M. A.; Hsieh, B. R. *Appl. Phys. Lett.* **1994**, *65*, 2030.

(8) (a) Meyer, H.; Haarer, D.; Naarmann, H.; Hörhold, H. H. *Phys. Rev. B* **1995**, *52*, 2587. (b) Blom, D. W. M.; de John, M. J. M.; Vleggaar, J. J. M. *Appl. Phys. Lett.* **1996**, *68*, 3308.

(9) (a) Yang, Y.; Pei, Q.; Heeger, A. J. *J. Appl. Phys.* **1996**, *79*, 934. (b) Wang, Y. Z.; Gebler, D. D.; Spry, D. J.; Fu, D. K.; Swager, T. M.; MacDiarmid, A. G.; Epstein, A. J. *IEEE Trans. Electron Devices* **1997**, *44*, 1263.

(10) (a) Li, X.-C.; Grimsdale, A. C.; Cervini, R.; Holmes, A. B.; Moratti, S. C.; Yong, T. M.; Grüner, J.; Friend, R. H. *ACS Symp. Ser.* **1997**, *672*, 322–344. (b) Meng, H.; Yu, W. L.; Huang, W. *Macromolecules* **1999**, *32*, 8841. (c) Martens, H. C. F.; Huiberts, J. N.; Blom, P. W. M. *Appl. Phys. Lett.* **2000**, *77*, 1852.

(11) Greenham, N. C.; Moratti, S. C.; Bradley, D. D. C.; Friend, R. H.; Holmes, A. B. *Nature (London)* **1993**, *365*, 628.

(12) Brown, A. R.; Bradley, D. D. C.; Burn, P. L. J.; Burroughes, H.; Friend, R. H.; Greenham, N.; Kraft, A. *Appl. Phys. Lett.* **1992**, *61*, 2793.

(13) Parker, I. D.; Pei, Q.; Marrocco, M. *Appl. Phys. Lett.* **1994**, *65*, 1272.

(14) Son, S.; Dodabalapur, A.; Lovinger, A. J.; Galvin, M. E. *Science* **1995**, *269*, 376.

(15) Strukelj, M.; Papadimitrakopoulos, F.; Miller, T. M.; Rothberg, L. J. *Science* **1995**, *267*, 1969.

(16) Peng, Z.; Bao, Z.; Galvin, M. E. *Chem. Mater.* **1998**, *10*, 2086.

(17) Zhou, X.; He, J.; Liao, L. S.; Lu, M.; Ding, X. M.; Hou, X. Y.; Zhang, X. M.; He, X. Q.; Lee, S. T. *Adv. Mater.* **2000**, *12*, 265.

(18) Kolb, E. S.; Gaudiana, R. A.; Mehta, P. G. *Macromolecules* **1996**, *29*, 2359.

(19) Greczmiel, M.; Strohriegl, P.; Meier, M.; Brtting, W. *Macromolecules* **1997**, *30*, 6042.

(20) (a) Liu, S.; Jiang, X.; Ma, H.; Liu, M. S.; Jen, K.-Y. *Macromolecules* **2000**, *33*, 3514. (b) Jung, B.-J.; Lee, J.-I.; Chu, H. Y.; Do, L.-M.; Shim, H.-K. *Macromolecules* **2002**, *35*, 2282.

(21) (a) Bellmann, E.; Shaheen, S. E.; Grubbs, R. H.; Marder, S. R.; Kippelen, B.; Peyghambarian, N. *Chem. Mater.* **1999**, *11*, 399. (b) Jiang, X.; Register, R. A.; Killeen, K. A.; Thompson, M. E.; Pschenitzka, F.; Sturm, J. C. *Chem. Mater.* **2000**, *12*, 2542.

(22) (a) Alam, M. M.; Jenekhe, S. A. *Chem. Mater.* **2002**, *14*, 4775. (b) Alam, M. M.; Tonzola, C. J.; Jenekhe, S. A. *Macromolecules* **2003**, *36*, 6577.

(23) (a) Yeh, K.-M.; Chen, Y. *J. Polym. Sci., Part A: Polym. Chem.* **2006**, *44*, 5362. (b) Ma, B.; Kim, B. J.; Deng, L.; Poulsen, D. A.; Thompson, M. E.; Frechet, J. M. J. *Macromolecules* **2007**, *40*, 8156. (c) Yeh, K.-M.; Chen, Y. *J. Polym. Sci., Part A: Polym. Chem.* **2007**, *45*, 2259.

(24) (a) Kreyenschmidt, M.; Klaerner, G.; Fuhrer, T.; Ashenhurst, J.; Karg, S.; Chen, W. D.; Lee, V. Y.; Scoot, J. C.; Miller, R. D. *Macromolecules* **1998**, *31*, 1099. (b) Grice, A. W.; Bradley, D. D. C.; Bernius, M. T.; Inbasekaran, M.; Wu, W. W.; Woo, E. P. *Appl. Phys. Lett.* **1998**, *73*, 629.

(25) (a) Scherf, U.; List, E. J. W. *Adv. Mater.* **2002**, *14*, 477. (b) Becker, S.; Ego, C.; Grimsdale, A. C.; List, E. J. W.; Marsitzky, D.; Pogantsch, A.; Setayesh, S.; Leising, G.; Müllen, K. *Synth. Met.* **2002**, *125*, 73.

(26) (a) Babel, A.; Jenekhe, S. A. *Macromolecules* **2003**, *36*, 7759. (b) Cho, N. S.; Hwang, D.-H.; Jung, B.-J.; Lim, E.; Lee, J.; Shim, H.-K. *Macromolecules* **2004**, *37*, 5265.

(27) Grice, A. W.; Tajbakhsh, A.; Burn, P. L.; Bradley, D. D. C. *Adv. Mater.* **1997**, *9*, 1174.

(28) (a) Adachi, C.; Baldo, M. A.; Forrest, S. R.; Thompson, M. E. *Appl. Phys. Lett.* **2000**, *77*, 904. (b) Chen, S.-H.; Chen, Y. *Macromolecules* **2005**, *38*, 53. (c) Yasuda, T.; Imase, T.; Nakamura, Y.; Yamamoto, T. *Macromolecules* **2005**, *38*, 4687.

(29) (a) Yamamor, A.; Adachi, C.; Koyama, T.; Taniguchi, Y. *Appl. Phys. Lett.* **1998**, *72*, 2147. (b) Mitschke, U.; Bäuerle, P. *J. Mater. Chem.* **2000**, *10*, 1471. (c) Ego, C.; Grimsdale, A. C.; Uckert, F.; Yu, G.; Srdanov, G.; Müllen, K. *Adv. Mater.* **2002**, *14*, 809.

(30) Coulson, D. R. *Inorg. Synth.* **1972**, *13*, 121.

(31) Ranger, M.; Rondeau, D.; Leclerc, M. *Macromolecules* **1997**, *30*, 7686.

(32) (a) Oishi, Y.; Ishida, M.; Kakimoto, M.; Imai, Y.; Kurosaki, T. *J. Polym. Sci., Part A: Polym. Chem.* **1992**, *30*, 1027. (b) Park, K. H.; Kakimoto, M.; Imai, Y. *J. Polym. Sci., Part A: Polym. Chem.* **1998**, *36*, 1987. (c) Hsiao, S.-H.; Chen, C.-W.; Liou, G.-S. *J. Polym. Sci., Part A: Polym. Chem.* **2004**, *42*, 3302.

(33) (a) Shu, C.-F.; Dodda, R.; Wu, F.-I.; Liu, M. S.; Jen, A. K.-Y. *Macromolecules* **2003**, *36*, 6698. (b) Wu, F.-I.; Shih, P.-I.; Shu, C.-F.; Tung, Y.-L.; Chi, Y. *Macromolecules* **2005**, *38*, 9028.

(34) (a) Barberis, V. P.; Mikroyannidis, J. A. *J. Polym. Sci., Part A: Polym. Chem.* **2006**, *44*, 3556. (b) Chien, C.-H.; Shih, P.-I.; Wu, F.-I.; Shu, C.-F.; Chi, Y. *J. Polym. Sci., Part A: Polym. Chem.* **2007**, *45*, 2073. (c) Yuan, M.-C.; Shih, P.-I.; Chien, C.-H.; Shu, C.-F. *J. Polym. Sci., Part A: Polym. Chem.* **2007**, *45*, 2925.

(35) Oelkrug, D.; Tompert, A.; Gierschner, J.; Egelhaaf, H.-J.; Hanack, M.; Hohloch, M.; Steinhuber, E. *J. Phys. Chem. B* **1998**, *102*, 1902.

(36) (a) Teetsov, J.; Fox, M. A. *J. Mater. Chem.* **1999**, *9*, 2117. (b) Becker, K.; Lupton, J. M.; Feldmann, J.; Nehls, B. S.; Galbrecht, F.; Gao, D. Q.; Scherf, U. *Adv. Funct. Mater.* **2006**, *16*, 364.

(37) Gong, X.; Ostrowski, J. C.; Moses, D.; Bazan, G. C.; Heeger, A. J. *Adv. Funct. Mater.* **2003**, *13*, 439.

(38) Uchida, M.; Adachi, C.; Koyama, T.; Taniguchi, Y. *J. Appl. Phys.* **1999**, *86*, 1680.

(39) Lee, Y.-Z.; Chen, X.; Chen, S.-A.; Wei, P.-K.; Fann, W.-S. *J. Am. Chem. Soc.* **2001**, *123*, 2296.

MA9004617